

Surface x-ray diffraction study of the Au(111) electrode in 0.01 M NaCl: Electrochemically induced surface reconstruction

B. M. Ocko, Alan Gibaud,^{a)} and Jia Wang

Department of Physics, Brookhaven National Laboratory, Upton, New York 11973

(Received 1 October 1991; accepted 24 February 1992)

The structure of the Au(111) electrode surface in a 0.01 M NaCl electrolyte has been investigated using grazing incident angle x-ray diffraction. The top layer of gold atoms undergoes a reversible phase transition between the (1×1) bulk termination and a $(p \times \sqrt{3})$ uniaxial discommensuration (striped) phase on changing the electrode potential. Below a critical potential the stripe separation, $p = 23$, is identical to vacuum measurements. At sufficiently positive potentials the surface forms an ideally terminated, (1×1) , Au(111) surface. Cycling the potential in the reconstructed region improves the reconstructed surface order.

I. INTRODUCTION

The understanding of surface structure in vacuum has progressed rapidly over the last several decades; many of the developments have been due to techniques involving electron probes. In electrochemistry, electrode surfaces are of fundamental importance, yet, very little is known about their *in situ* structure. In part, this is due to the inability of electrons to penetrate solutions. With the availability of high brightness synchrotron sources surface x-ray diffraction has become a viable method to study *in situ* structure.¹⁻⁴

In vacuum, the Au(111) surface reconstructs to form a uniaxial compressed surface phase.⁵⁻⁸ Under electrochemical conditions, the surface charge at the Au(111) surface can be varied continuously and reversibly by as much as 0.5 electrons per surface atom. Very little is known about the atomic structure of the Au(111) electrode surface. In this paper we report the results of an x-ray scattering study of the $(23 \times \sqrt{3})$ reconstruction of the Au(111) electrode surface in 0.01 M NaCl. A full description of the phase behavior and kinetic effects of the Au(111) surface in a variety of salt solutions is reported elsewhere.⁹ In order to differentiate the respective roles of surface charge and adsorbates, studies were carried out in 0.1 M solutions of NaF, NaCl, and NaBr as reported in Refs. 9 and 10. The phase transition occurs at an induced surface charge density of $0.07 \pm 0.02 e/\text{atom}$ in all three 0.1 M solutions.^{9,10}

A current survey of the gold electrode literature can be found in a recent review article.¹¹ In the following, we review some of the significant studies at the Au(111) face. The possibility that electrochemically induced reconstructions of gold surfaces might exist was proposed by Hamelin based on the hysteresis observed in capacity-potential curves at the same potential where a peak emerged in cyclic voltammograms (current voltage curves).^{12,13} *Ex situ* low-energy electron diffraction (LEED) studies by Kolb Schneider have shown that the Au(111) surface, after emersion from an electrochemical cell, forms a $(23 \times \sqrt{3})$ phase in the negative potential regime.¹⁴ Recent *ex situ* LEED studies by Ross and D'Agostino have confirmed that gold surfaces remain reconstructed after emersion.¹⁵ For the case of the Au(001) surface in HClO₄, *in situ*

electroreflectance measurements provided further evidence that gold electrodes reconstruct.¹⁴ Second harmonic generation (SHG) measurements at the Au(111) surface^{16,17} have demonstrated that the phase transition between the $(23 \times \sqrt{3})$ and (1×1) phase can be monitored *in situ* by the additional symmetry pattern in the SHG intensity associated with the uniaxial compressed phase. However, it is difficult to extract detailed structural information from these measurements. Concurrent with the present surface x-ray scattering (SXS) study, *in situ* scanning tunneling microscopy (STM) studies^{18,19} in HClO₄ solutions have confirmed the existence of the $(p \times \sqrt{3})$ reconstruction within the negative potential regime. In the present electrochemical x-ray scattering study, the characteristic stripe separation—averaged over a macroscopic area—versus the applied potential has been measured with a lateral resolution which exceeds the capability of current STM measurements.

Our understanding of the Au(111) surface in vacuum has been obtained from a variety of techniques including LEED,^{6,7} transmission electron diffraction (TED),²⁰ helium scattering,²¹ surface x-ray diffraction,^{8,22} and from STM.^{23,24} The observed diffraction peaks have been interpreted as a rectangular $(23 \times \sqrt{3})$ unit cell corresponding to a uniaxial compression (4.4%) along the $\langle 100 \rangle$ direction in hexagonal coordinates (see Sec. II B) as shown in Fig. 1(a). This structure is often referred to as a stripe-domain phase where the stripe separation is proportional to the inverse compressibility. From TED measurements,²⁰ helium scattering,²¹ and from x-ray reflectivity techniques⁸ it has been inferred that the surface atoms are arranged in a manner such that the surface stacking sequence changes between ABC to ABA as shown in Fig. 1(a). Recent x-ray scattering⁸ and STM studies^{23,24} have shown that the discommensuration direction rotates by $\pm 60^\circ$ to form a regular array of kink dislocations in the discommensuration direction under vacuum conditions. Under electrochemical conditions with STM, similar kinks in the discommensuration direction have been observed at the Au(111) electrode in HClO₄ solutions at negative potentials.^{18,19}

In the present study we have characterized the in-plane structure of the Au(111) surface versus potential in 0.01 M NaCl. We have utilized a salt solution instead of the

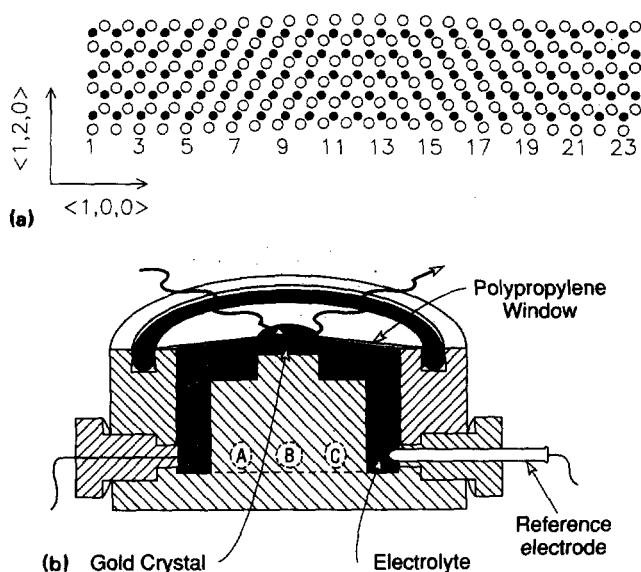


FIG. 1. (a) In-plane hexagonal structure of the Au(111) surface. The solid (filled) circles correspond to atoms in the second (first) layer. Surface atoms in the left and right hand sides of the figure are in undistorted hexagonal sites (ABC stacking sequence) whereas in the center of the figure the atoms are in faulted sites (ABA stacking sequence). (Refs. 21, 22) For 24 surface atoms in place of 23 underlying surface atoms, the compression is $24/23 - 1 = 4.4\%$ and $\delta = (\sqrt{3}/2)/23 = 0.038$. (b) X-ray scattering electrochemical cell. The Au(111) single crystal is held at the top center by a Kel-F clamp. The cell is sealed with a polypropylene window by an o-ring. (A) electrolyte input, (B) counter electrode, (C) electrolyte output. An outer chamber (not shown) is filled with nitrogen gas to prevent diffusion of oxygen through the polypropylene window.

more commonly used acid solutions. Under these conditions we obtain a wider double layer potential range and are able to determine whether cations have any effects on the structure of the Au(111) surface. The latter is not possible in acid solutions since the cation is always a proton. At sufficiently positive potentials the stripe-phase reconstruction vanishes and the diffraction pattern exhibits the symmetry of the underlying lattice. The phase transition is reversible although there are significant hysteresis effects. A comprehensive study of the Au(111) surface in NaF, LiCl, NaCl, KCl, CsCl, and NaBr electrolytes with concentrations ranging between 0.01 and 0.1 M is reported elsewhere.⁹

II. EXPERIMENTAL TECHNIQUES

A. Electrochemical and surface preparation

Gold disk electrodes (2 mm by 10 mm diam) were sliced from a common single crystal, and aligned along the nominal $\langle 111 \rangle$ direction using a wire spark cutter. These disks were aligned and sanded with the $\langle 111 \rangle$ planes oriented within 0.1° of the surface normal axis \hat{n} . The disks were mechanically polished with $6 \mu\text{m}$ diamond paste followed by $1 \mu\text{m}$ alumina powder. Although the surface has a mirror finish, the mechanical polishing creates microscopic surface damage. In order to expose undamaged $\langle 111 \rangle$ planes, the samples were electrochemically polished in 1:1:1 (volume) HCl:ethylene glycol:ethanol.²⁵ The final surface preparation step involved sputtering with argon at

5×10^{-5} Torr at 800°C using a defocused beam at 2 kV and $2 \mu\text{A}$ for several hours. The sample was transferred through air to an electrochemical x-ray scattering cell constructed from Kel-F³ as shown in Fig. 1(b).

A $6 \mu\text{m}$ polypropylene window covers and seals the cell with a thin capillary electrolyte film between the crystal face and the polypropylene film. An outer chamber was flushed with N_2 gas to prevent oxygen from diffusing through the polypropylene membrane. The applied potential was referenced to an Ag/AgCl(3 M KCl) electrode connected to the cell through a micro glass frit. Counter electrodes were either gold or platinum wires.

The electrolyte solutions were prepared from superpure NaCl diluted with ultrapure H_2O . The diluted electrolyte solutions were deoxygenated with 99.999% N_2 gas immediately before filling the cell. After flushing the cell with N_2 gas, the deoxygenated electrolyte was injected into the cell through a syringe with the control potential turned off. The cell was filled with enough solution to expand the polypropylene window leaving a thick electrolyte layer (several mm) between the face and the window. Cyclic voltammograms were carried out in this geometry to check the electrochemical conditions of the cell. Before carrying out the x-ray scattering measurements the cell was deflated which leaves a thin electrolyte layer which we estimate from the small angle reflectivity measurements to be between 10 and $20 \mu\text{m}$ thick. In the thin electrolyte layer geometry, the effects of bulk impurities are greatly reduced relative to the thick electrolyte geometry.

Our studies of the Au(111) surface were carried out in a potential range which is referred to the "double layer" region. Within this potential range there are no Faradaic processes and the electrode can be treated as an ideally polarizable interface. We note that the potential region in which this approximation is valid is bounded by hydrogen evolution at negative potentials and gold oxidation processes at positive potentials. In salt solutions (pH about 6), hydrogen evolution occurs below -0.8 V . The high potential limit was 0.8 V .

B. X-ray techniques

The x-ray scattering measurements reported in this paper were carried out with focused, monochromatic synchrotron radiation at beam line X22B at the National Synchrotron Light Source (NSLS) at Brookhaven National Laboratory. In the four circle geometry the sample orientation is oriented through its Euler angles θ , χ , and ϕ ²⁶ by a spectrometer under computer control. The scattering wave vector magnitude is $|\mathbf{k}_f - \mathbf{k}_i| = 4\pi/\lambda \sin(2\theta/2)$ where \mathbf{k}_i and \mathbf{k}_f correspond to the incident and scattered wave vectors and where 2θ is the detector angle within the scattering plane. Diffraction measurements are carried out by measuring the scattering intensity along paths in reciprocal space (see below).

Measurements were carried out at an energy corresponding to a wavelength of $\lambda = 1.54 \text{ \AA}$ at beamline X22B. The scattered intensity is measured with a scintillator detector placed on the 2θ arm and is normalized to the incident flux. At grazing incidence, i.e., small α , the incident x

rays illuminate a region of the crystal 0.5 mm wide across the entire crystal face (10 mm). The scattering resolution, in reciprocal space, is primarily determined by the angular acceptance of the scattered radiation and the quality of the mosaic of the Au(111) crystal. The illuminated area of the incident beam does not directly affect the resolution. For the present measurements, the resolution within the scattering plane was determined by an array of equally spaced parallel plates (Soller slits) which provide a 2θ resolution of 0.1° half-width at half-maximum (HWHM). This corresponds to a longitudinal in-plane resolution in reciprocal space of 0.007 \AA^{-1} HWHM at $\lambda = 1.54 \text{ \AA}$. The transverse in-plane resolution is limited by the mosaic spread of the crystalline order which is typically 0.025° HWHM. Normal to the scattering plane, the resolution is determined by ψ_2 , which is set by 10 mm detector slits located on the four circle 2θ arm which is 600 mm from the sample position.

The two principle features of the diffraction pattern from the Au(111) surface in reciprocal space are Bragg reflections and weak streaks of scattering along the surface normal direction.²⁷⁻²⁹ In order to describe the scattering wave vector in terms of its components in the surface plane and along \hat{n} it is convenient to use a hexagonal coordinate system.^{8,30,31} The hexagonal reciprocal space position is represented by the vector (H,K,L) or (H,K) within the surface plane where

$$a^* = b^* = \frac{4\pi}{\sqrt{3}a} = 2.52 \text{ \AA}^{-1}, \quad c^* = \frac{2\pi}{\sqrt{6}a} = 0.89 \text{ \AA}^{-1}.$$

The nearest-neighbor separation, a , equals 2.885 \AA .

The relationship between the cubic vector, $(h,k,l)_{\text{cubic}}$ and the hexagonal vector (H,K,L) is given by the transformations $h = -4H/3 - 2K/3 + L/3$, $k = 2H/3 - 2K/3 + L/3$, and $l = 2H/3 + 4K/3 + L/3$. For example, $(1,1,1)_{\text{cubic}} = (0,0,3)$, $(0,0,2)_{\text{cubic}} = (0,1,2)$, and $(0,2,2)_{\text{cubic}} = (1,0,4)$. The vector $(H,K,0)$ lies within the surface plane whereas $(0,0,L)$ is along the surface normal direction.

A principle feature of the Au(111) surface reconstruction (in vacuum) is a uniaxial compression of the top layer of gold atoms by 4.4% as shown in Fig. 1(a). This picture has been inferred from scattering techniques including low-energy electron diffraction (LEED),^{6,7} transmission electron diffraction (TED),²⁰ helium scattering,²¹ and surface x-ray diffraction studies.⁸ In an x-ray scattering measurement the $(p \times \sqrt{3})$ reconstruction gives rise to additional rods of scattering. We refer to these rods of scattering as over-layer reflectivity since the scattering originates from the reconstructed "overlayer" (top layer).^{8,32} These over-layer reflections (modulation peaks) are arranged in a hexagonal pattern surrounding the integer (H,K) positions and the magnitude of the modulation wave vector is given by δa^* . Their projection on the surface plane is shown in Fig. 2. These additional reflections originate from the compression of the top layer along the three $\sqrt{3}$ directions in reciprocal space.

The discommensuration periodicity, p , is defined as $\sqrt{3}/(2\delta)$. For example, if there are 24 surface atoms in place of 23 underlying surface atoms, the compression is $24/23 - 1$

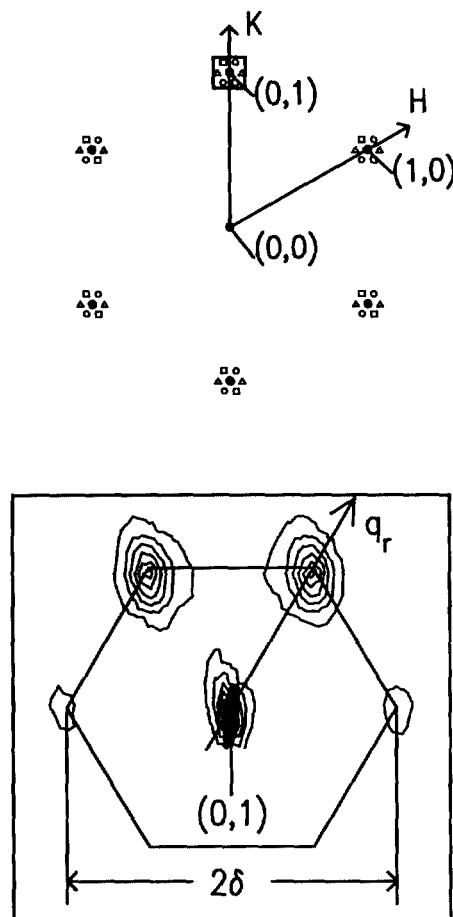


FIG. 2. Top: In-plane diffraction pattern of the Au(111) $(23 \times \sqrt{3})$ reconstruction in hexagonal coordinates. The solid circles are at the periodicities from the underlying bulk substrate. The open symbols originate from the $(23 \times \sqrt{3})$ reconstructed phase with three rotationally equivalent domains. The axis q_r is defined to be along the $(1,1)$ direction. Bottom: X-ray scattering equal intensity contours in the vicinity of the $(0,1)$ reflection at $L = 0.5$ measured in 0.01 M NaCl at -0.3 V vs a saturated Ag/AgCl.

$= 4.4\%$ and $\delta = \sqrt{3}/2/23 = 0.038$. In an x-ray scattering experiment in which the intensity is collected over several square mm, all three symmetry equivalent domains are probed. At sufficiently positive applied potentials, in all electrolytes, the scattering from the Au(111) surface does not exhibit the diffraction pattern of a reconstructed surface. Instead, only the integral reflections (H,K) originating from the substrate are observed.

III. RESULTS

The in-plane diffraction pattern from the Au(111) surface, obtained within the reconstructed potential regime, is virtually identical in all electrolytes.⁹ In the present paper we report the potential dependence of x-ray scattering measurements from the Au(111) surface in 0.01 M NaCl. Below a critical threshold potential, the scattering exhibits the characteristic diffraction pattern of a $(p \times \sqrt{3})$ striped phase with three rotationally equivalent domains. In the bottom panel of Fig. 2, equal intensity contours are shown in the vicinity of the $(0,1)$ reflection at $L = 0.5$ for 0.01 M

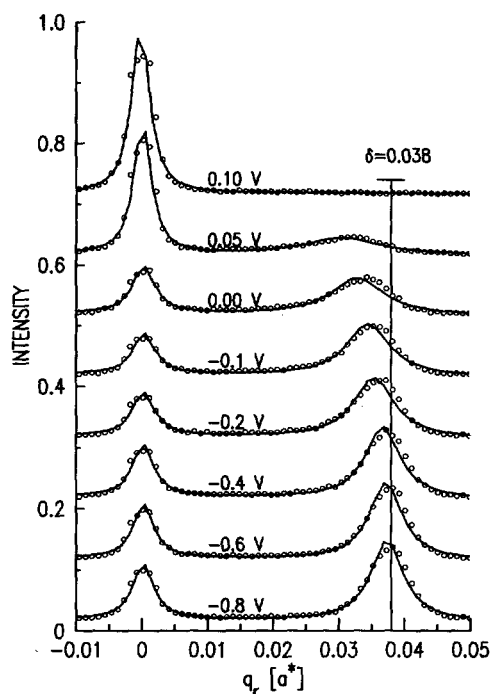


FIG. 3. Representative x-ray scattering scans along the q_r axis (see Fig. 2) for the Au(111) surface at $L = 0.2$ in 0.01 M NaCl solution at a series of potentials chosen from scans between 0.1 and -0.8 V in steps of -0.05 V. The solid lines are fits to a Lorentzian line shape described in the text.

NaCl at -0.3 V. Four peaks surrounding the (0,1) reflection are arranged in a hexagonal pattern, where $\delta = 0.038$ is the length of the hexagon side in dimensionless units.^{6,7,20-22} Our electrochemical measurements of the incommensurability are in good agreement with high resolution vacuum measurements at $T = 300$ K, where $\delta = 0.0383$.^{6,7,20,21} Figure 2 shows that the two surface reflections at largest wave vector transfer, from the origin, are the most intense and that the two reflections with the smallest wave vector transfer are not observed. These difference can be attributed to the arrangement of atoms in the reconstructed unit cell (structure factor).

We have carried out a detailed study of the potential dependence of the scattering from the Au(111) surface through the (0,1) reflection along the $\langle 1,1 \rangle$ direction which we label as the q_r axis in Fig. 2. Along the q_r axis, the in-plane projection of the scattering wave vector is given by $(q_r/\sqrt{3}a^*, 1 + q_r/\sqrt{3}a^*)$. In Fig. 3, we present the measured scattering intensity obtained along the q_r axis at $L = 0.2$ at a series of decreasing potentials between 0.1 and -0.8 V with an effective scan rate of 0.5 mV/s. Above 0.10 V the scattering is centered at $q_r = 0$ (Fig. 3) corresponding to the (0,1) bulk reflection. As the potential is reduced below 0.05 V, the intensity of the reconstruction peaks grows. Concomitantly, the (0,1) reflection decreases in intensity but remains centered at zero. The position of the reconstruction peak moves outward (increasing compression) as the potential is decreased. The maximum scattering intensity at (0,1) is about thirty times the diffuse scattering originating from the electrolyte and window.

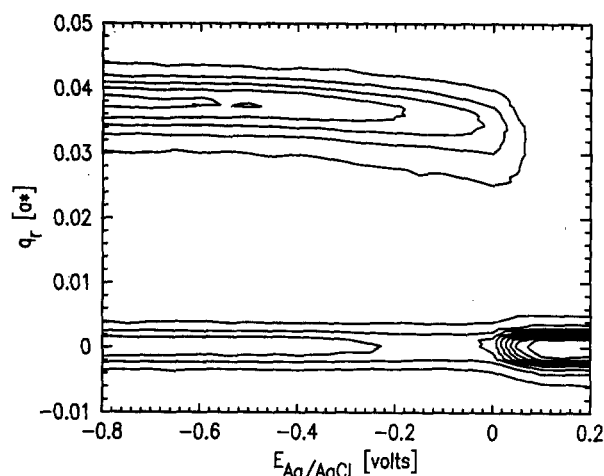


FIG. 4. Equal intensity contours created from the intensity distribution along q_r , starting at a potential of 0.2 V and extending to -0.8 in steps of 0.05 V. The emergence of a broad peak at $q_r = 0.030a^*$ corresponds to the formation of the reconstructed phase.

An alternative approach for displaying the potential dependence of the surface scattering—shown as a series of displaced curves in Fig. 3—is shown in Fig. 4 as a contour plot. The intensity matrix, used to create the contour plot, was formed by measuring the scattered intensity along q_r at a series of decreasing potentials starting at a potential of 0.2 V and extending to -0.8 in steps of 0.05 V. It is apparent from Fig. 4 that the reconstructed phases starts to form at 0.05 V as indicated by the emergence of contour lines at $q_r = 0.030a^*$. As the potential is further decreased the reconstruction wave vector moves outward to $q_r = 0.038a^*$ ($p = 23$) and the scattering line shape narrows corresponding to an increased surface order.

To extract additional information from the scattering profiles, we have fit the scattering profiles along q_r to the sum of two Lorentzians and a small background

$$S(q_r) = \frac{I_0}{1 + q_r^2/\sigma^2} + \frac{I_\delta}{1 + (q_r - \delta)^2/\sigma_\delta^2} + A + Bq_r/a^*. \quad (1)$$

The first term represents the scattering at the substrate (0,1) wave vector, the second term corresponds to the scattering centered at $(\delta/\sqrt{3}, 1 + \delta/\sqrt{3})$, and A and B are small background parameters. The parameters I_0 and I_δ correspond to the peak intensities at q_r equal to 0 and δ , respectively. The Lorentzian profile widths in Eq. (4) are σ and σ_δ . In reciprocal space, the Lorentzian line shape is derived from a one-dimensional real space atomic model in which the correlation function decays exponentially with a length $\zeta_\delta = a\sqrt{3}/(4\pi\sigma_\delta)$. This length is a measure of the distance over which atoms in the reconstructed layer are positionally correlated. The discommensuration periodicity, which we also refer to as the stripe separation, $L_\delta = pa = a\sqrt{3}/(2\delta)$.

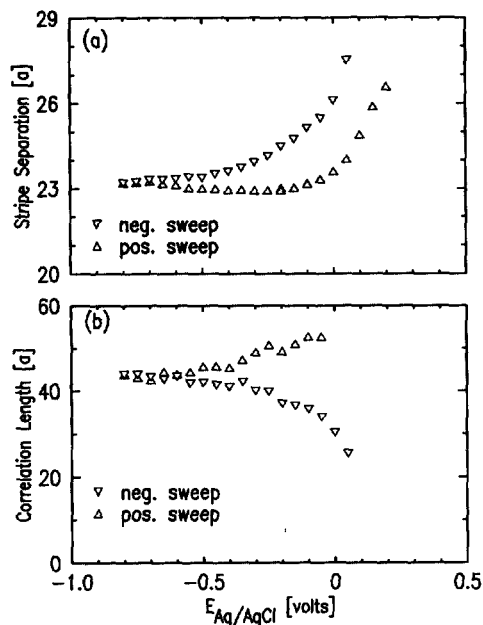


FIG. 5. The stripe separation (a) and correlation length (b) obtained by fitting the data shown in Figs. 3 and 4 to Eq. (1) for the Au(111) surface in 0.01 M NaCl. The triangles and upside down triangles correspond to positive and negative sweep directions, respectively.

In an x-ray scattering measurement, the correlation length of the underlying Au(111) facets can also be determined from the inverse peak widths in reciprocal space. If the surface is composed of terraces (facets) separated from each other by monoatomic steps, the scattering from neighboring facets adds out-of-phase at the (0,1) reflection and the peak width is broadened by this effect. For an exponential facet size distribution, the mean facet size along the $\langle 1,1 \rangle$ direction ζ equals $a\sqrt{3}/(4\pi\sigma)$. In the present set of measurements, ζ is at least 300 Å and represents a lower bound for the distance between steps. Incorporating finite resolution effects into the analysis increases the effective facet size.

In the fitting procedure the peak position δ the widths, σ and σ_δ , the amplitudes, I_0 and I_δ , and the background are varied for the scattering profiles at constant potential. Instrumental resolution effects have not been included in the present analysis since improving the reciprocal space resolution by a factor of ten did not modify the observed scattering linewidths.³³ The scattering in the wings of the peak at $q_r = 0$ (substrate periodicity) exhibit a q_r^{-2} fall off. At small q_r , however, the scattering profiles are not adequately represented by the model. In part, this discrepancy is due to finite substrate mosaic effects which have a Gaussian component that is not included in our Lorentzian model. At $q_r = 0.038a^*$ (reconstructed periodicity) the scattering is reasonably well represented by the Lorentzian profiles at sufficiently negative potentials.

The stripe separation L_δ and the correlation length ζ_δ obtained from fits to Eq. (1) are shown in Figs. 5(a) and 5(b), respectively as a function of the applied potential. The potential cycle originates at 0.1 V and continues to -0.8 V and then back to 0 V in steps of 0.05 V. After the

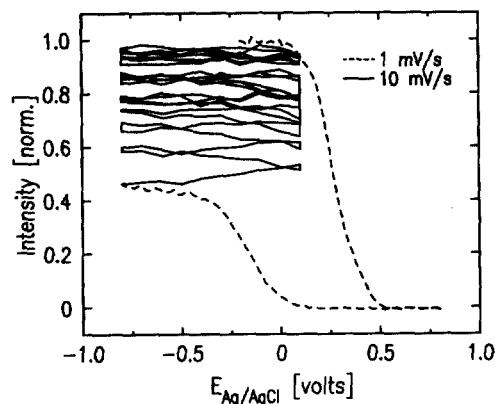


FIG. 6. The effect of surface grooming (see text) at the Au(111) surface in 0.1 M NaF. The data is acquired at fixed scan rates of 1 and 10 mV/s. (see key) at a wave vector $(0.038/\sqrt{3}, 1 + 0.038/\sqrt{3}, 0.2)$. At this position the scattered intensity increases as the stripe length L_δ approaches 23 and as the correlation length increases. The scattered intensity increases during potential cycles between -0.8 and 0.1 V.

initial signs of the surface reconstruction at 0.05 V, corresponding to the emergence of the modulation peak, there is a continued compression as the potential is decreased, as shown by the inverted triangles in Fig. 5(a). The maximum compression corresponds to a stripe periodicity of $23a$. Changes in the reconstructed surface structure virtually cease below -0.6 V. Further compression and an increase in the correlation length resumes after sweeping the potential positive. The stripe domain correlation length ζ_δ achieves a maximum value of $55a$ at -0.1 V. This is at a potential just below where the lifting of reconstruction starts and ζ_δ is always less than ζ .

In vacuum, the Au(111) surface forms an ordered array of 60° shifts in the discommensuration direction.²²⁻²⁴ For the Si(111) surface an ordered array of reconstructed domains with different orientations reduces²² the strain energy of the underlying substrate. This argument may also apply to the Au(111) surface.³⁴ These shifts in the discommensuration direction (kinks) for the Au(111) surface are separated by about $80a$ at $T = 300$ K. This new wave vector, $\sim 2\pi/80a$, gives rise to additional diffraction spots.⁸ At the electrode surface, at all potentials, these additional diffraction spots are absent. Hence, there is no evidence that the kinks form an ordered array. However, the Au(111) electrode surface may form a disordered array of kinks in which the kink spacing is irregular. This observation is consistent with recent *in situ* STM studies of the Au(111) surface in HClO_4 .^{18,19} These studies clearly establish the existence of discommensuration kinks, however, a well ordered array of kinks can not be ascertained from the present STM results.

In 0.01 M NaCl solutions, the correlation length can be increased by cycling the potential in the reconstructed potential region. We refer to the surface state where the maximum compression and correlation length are achieved as the "groomed" surface. The effect of surface grooming on the Au(111) surface is shown in Fig. 6 by recording the scattered intensity while the potential is swept at fixed rates

in both sweep directions. The spectrometer is set to $(0.038/\sqrt{3}, 1 + 0.038/\sqrt{3}, 0.2)$. At this position the scattered intensity increases as the stripe length L_s approaches 23 and as the correlation length increases. The effect of surface grooming on the Au(111) surface in 0.1 M NaF is shown in Fig. 6. Similar results have been obtained in 0.01 M NaCl. In Fig. 6, the normalized scattered intensity has been obtained by dividing the scattered intensities by the maximum scattered intensity recorded in the grooming procedure. In the figure, the first potential ramp starts at 0.8 V and stops at -0.8 V at a rate of 1 mV/s. The groomed surface is obtained by repeated potential cycles between 0.8 and 0.1 V at a rate of 10 mV/s. Finally, the potential is swept from -0.2 to 0.8 V at a sweep rate of 1 mV/s. In the first potential ramp the normalized intensity only reaches 45% (dashed line) of the groomed value. During the grooming cycles (solids lines) between -0.8 and 0.1 V the intensity increases substantially. After 20 grooming cycles (1 h) there is no further increase in the intensity at $(0.038/\sqrt{3}, 1 + 0.038/\sqrt{3}, 0.2)$. For the studies in 0.01 M NaCl, cycling the potential for several days in the reconstructed potential region did not improve the correlation length beyond $55a$. In conjunction with specular reflectivity measurements, which are sensitive to the surface normal structure,⁹ we know that the grooming process only involves a rearrangement of the atoms within the surface plane. Finally, the grooming process may facilitate a rearrangement of the discommensuration kinks which leads to a more ordered surface.

Complementary information on the Au(111) surface structure can be obtained by monitoring the potential dependence of the scattering at several positions along the rods of scattering. Different positions in reciprocal space are sensitive to different aspects of the surface structure and likewise the potential dependence varies with reciprocal space position. For instance, scattering with an in-plane wave vector (0,1) couples to the Fourier transform of the atomic density distribution within the surface plane at a wave vector corresponding to the undistorted bulk hexagonal spacing. Also the scattering at the reconstructed position increases with decreasing potential, whereas the scattering at (0,1,0.5) increases when the reconstruction is lifted at positive potentials. These differences have motivated us to present the potential dependence at different reciprocal space positions

Figure 7 displays the potential dependence of the scattering from the Au(111) surface in 0.01 M NaCl at (a) $(0.038/\sqrt{3}, 1 + 0.038/\sqrt{3}, 0.2)$, and at (b) (0,1,0.5). Each panel corresponds to a potential cycle starting at 0.6 to -0.8 V and then back to 0.6 V at a sweep rate of 1.0 mV/s. In the top panel [Fig. 7(a)] the scattering intensity corresponds to the principle $(23 \times \sqrt{3})$ reconstruction peak. We have subtracted the diffuse background and normalized the intensity to the groomed state. At 0.05 V the intensity at $(0.038/\sqrt{3}, 1 + 0.038/\sqrt{3}, 0.2)$ starts to increase corresponding to the formation of the reconstructed phase. Note that the maximum scattered intensity is achieved in the positive going potential sweep before the reconstructed

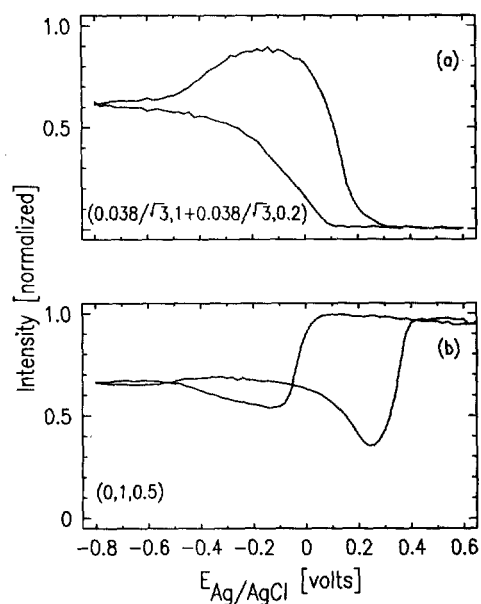


FIG. 7. Potential dependence of the x-ray scattering intensities at (a) $(0.038/\sqrt{3}, 1 + 0.038/\sqrt{3}, 0.2)$, and (b) (0,1,0.5) in 0.01 M NaCl solution. Data was acquired at a scan rate of 1 mV/s. in both the negative and positive slew directions as indicated by the arrows in the figures. In all cases the potential cycles start at 0.6 V. The background subtracted intensities are normalized to unity at their maximum values.

phase is lifted. The measured intensity at $(0.038/\sqrt{3}, 1 + 0.038/\sqrt{3}, 0.2)$ does not always reflect the peak intensity along q_r , since δ varies with potential as shown in Fig. 3. Despite this fact, the potential dependence at this position does provide a reasonable measure of the reconstructed order parameter. This is because the peak profiles are relatively broad compared to the changes in δ with potential.

The scattering at (0,1,0.5) versus the applied potential is shown in Fig. 7(b) where the scattering intensity has been normalized to unity at 0.6 V. This reciprocal space position is exactly halfway between the (0,1, $\bar{1}$), and (0,1,2) Bragg peaks. At these halfway positions, the measured intensities are most sensitive to effects of surface disorder. In the (1×1) potential region between 0.4 and 0.6 V there is no change in the intensity with potential as shown in Fig. 7(b). As discussed in the context of the nonspecular reflectivity profiles at the Au(111) surface⁹ this strongly suggests that the lateral position of the gold atoms in the top atomic layer remains fixed within this potential region. At the lowest potentials the surface is reconstructed and the intensity at (0,1,0.5) falls to about 65% of the (1×1) value. Comparing the scattering at (0,1,0.5) with the scattering at $(0.038/\sqrt{3}, 1 + 0.038/\sqrt{3}, 0.2)$ versus potential allows us to draw several interesting conclusions. The sharp break in slope at 0.05 V at $(0.038/\sqrt{3}, 1 + 0.038/\sqrt{3}, 0.2)$ (negative potential sweep) is clearly correlated with the sharp break in slope at (0,1,0.5) corresponding to the loss of order at the in-plane wave vector (0,1). In the positive sweep direction, the loss of the reconstructed order is nearly complete by 0.25 V, Fig. 7(a), whereas the order at the (0,1) wave vector is not completely restored until 0.40 V. A dip in the scattering

intensity at (0,1,0.5) appears in Fig. 7(b) during both scan directions. In the positive sweep direction this effect is most pronounced and the intensity at 0.25 V falls to 35% of the intensity at 0.6 V. We believe that this dip in the scattering intensity (0.25 V) corresponds to increased surface disorder during the lifting of the reconstructed phase.

IV. CONCLUSIONS

In this article we have presented the results of *in situ* structural x-ray scattering studies of the Au(111) electrode surface in 0.01 M NaCl solutions. The top layer of gold atoms undergoes a reversible phase transition between the (1×1) bulk termination and a ($p \times \sqrt{3}$) uniaxial (striped) discommensuration phase on changing the electrode potential. Below a critical potential the stripe separation, $p = 23$, is identical to results obtained in vacuum. An ordered array of discommensuration kinks is not observed. At sufficiently positive potentials the striped phase disappears and the surface exhibits the structure of a (1×1) surface.

In a separate paper, a comprehensive x-ray scattering and reflectivity study of the Au(111) surface is reported in a variety of salt electrolytes.⁹ The potential dependence of the scattered intensity is a strong function of the electrolyte anion species. However, in all these solutions, the transition between the (1×1) and reconstructed surfaces occurs at a common value of the surface charge. In particular, the reconstruction starts to form and lift at a negative charge of 0.07 electrons per surface gold atom. Additional information on the nature of the reconstruction has been obtained by measuring the transition kinetics after a step change in the potential.

ACKNOWLEDGMENTS

The authors thank Hugh Isaacs and Alison Davenport for their assistance. This work has been supported by an exploratory research grant at Brookhaven National Laboratory and by the Division of Materials Research, U. S. Department of Energy, under Contract No. DE-AC02-76CH00016.

This article was presented at the 38th National Symposium of the American Vacuum Society Topical Conference, Surface Science at the Solid-Liquid Interface (TC1).

^aUniversity of Maine, U.A. 807, C.N.R.S., Le Mans, France

¹M. F. Toney and O. R. Melroy, in *In-Situ Studies of Electrochemical Interfaces*, edited by H. D. Abruna (VCH Verlag Chemical, Berlin, 1991).

- ²O. R. Melroy, M. F. Toney, G. L. Borges, M. G. Samant, L. Blum, J. B. Kortright, P. N. Ross, and L. Blum, *Phys. Rev. B* **38**, 10962 (1988).
- ³B. M. Ocko, Jia Wang, Alison Davenport, and Hugh Isaacs, *Phys. Rev. Lett.* **65**, 1466 (1990).
- ⁴C. A. Melendres, H. You, V. A. Maroni, Z. Nagy, and W. Yun, *J. Electroanal. Chem.* **297**, 549 (1991).
- ⁵M. A. Van Hove, R. J. Koestner, P. C. Stair, J. B. Biberian, L. L. Kesmodel, I. Bartos, and G. A. Somorjai, *Surf. Sci.* **103**, 189 (1981).
- ⁶J. Perdureau, J. P. Biberian, and G. E. Rhead, *J. Phys. F* **4**, 1978 (1974).
- ⁷D. M. Zehner and J. F. Wendelken, *Proceedings of the Seventh International Vacuum Congress and the Third International Conference on Solid Surfaces*, Vienna, 1977 (F. Berger and Sohne, Vienna, 1977), p. 517.
- ⁸A. R. Sandy, S. G. J. Mochrie, D. M. Zehner, K. G. Huang, and D. Gibbs, *Phys. Rev. B* **43**, 4667 (1991).
- ⁹J. Wang, B. M. Ocko, A. J. Davenport, and H. S. Isaacs, *Phys. Rev. B* **46** (1992).
- ¹⁰J. Wang, A. J. Davenport, H. S. Isaacs, and B. M. Ocko, *Science* **255**, 1416 (1992).
- ¹¹D. M. Kolb, in *Frontiers in Electrochemistry*, edited by J. Lipowski and P. N. Ross (VCH, New York, 1991), Vol. 2.
- ¹²A. Hamelin, *J. Electroanal. Chem.* **142**, 299 (1982).
- ¹³J. P. Bellier and A. Hamelin, *C. R. Acad. Sci.* **280**, 1489 (1975).
- ¹⁴D. M. Kolb and J. Schneider, *Electrochimica Acta* **31**, 929 (1986).
- ¹⁵P. N. Ross, Jr. and A. T. D'Agostino, *Electrochim. Acta* **37**, 615 (1992).
- ¹⁶A. Friedrich, B. Pettinger, D. M. Kolb, G. Lüpke, R. Steinhoff, and G. Marowsky, *Chem. Phys. Lett.* **163**, 123 (1989).
- ¹⁷G. Lüpke, G. Marowsky, R. Steinhoff, A. Friedrich, B. Pettinger, and D. M. Kolb, *Phys. Rev. B* **41**, 6913 (1991).
- ¹⁸N. J. Tao and S. M. Lindsay, *J. Appl. Phys.* **170**, 5143 (1991).
- ¹⁹X. Gao, A. Hamelin, and M. J. Weaver, *J. Chem. Phys.* **95**, 6993 (1991).
- ²⁰K. Yamazaki, K. Takayamagi, Y. Tanishiro, and K. Yagi, *Surf. Sci.* **199**, 595 (1988).
- ²¹U. Harten, A. M. Lahee, J. Peter Toennies, and Ch. Woll, *Phys. Rev. Lett.* **54**, 2619 (1985).
- ²²K. G. Huang, D. Gibbs, D. M. Zehner, A. R. Sandy, and S. G. J. Mochrie, *Phys. Rev. Lett.* **65**, 3317 (1990).
- ²³J. V. Barth, H. Brune, G. Ertl, and R. J. Behm, *Phys. Rev. B* **42**, 9307 (1990).
- ²⁴D. D. Chambliss and R. J. Wilson, *J. Vac. Sci. Technol. B* **9**, 928 (1991).
- ²⁵J. L. Whitton and J. A. Davies, *J. Electrochem. Soc.* **111**, 1347 (1964).
- ²⁶W. R. Busing and H. A. Levy, *Acta. Crystallogr.* **22**, 454 (1967).
- ²⁷I. K. Robinson, *Phys. Rev. B* **33**, 3830 (1986).
- ²⁸A. M. Afanas'ev, P. A. Aleksandrov, S. S. Fanchenko, V. A. Chaplanov, and S. S. Yakimov, *Acta. Crystallogr. A* **42**, 116 (1986).
- ²⁹S. R. Andrews and R. A. Cowley, *J. Phys. C* **18**, 6427 (1985).
- ³⁰J. Bohr, R. Feidenhans'l, M. Nielsen, M. Toney, R. L. Johnson, and I. K. Robinson, *Phys. Rev. Lett.* **54**, 1275 (1985).
- ³¹B. E. Warren, *X-ray Diffraction* (Addison-Wesley, Reading, MA, 1969).
- ³²B. M. Ocko, D. Gibbs, K. G. Huang, D. M. Zehner, and S. G. J. Mochrie, *Phys. Rev. B* **44**, 6429 (1991).
- ³³This was carried out by using a Ge(111) analyzer rather than Soller slits.
- ³⁴O. L. Alerhand, D. Vanderbilt, R. D. Meade, and J. D. Joannopoulos, *Phys. Rev. Lett.* **61**, 1973 (1988).